Methods

Two-hybrid screening

We used the Matchmaker Two-Hybrid system (Clontech). DNA coding the proline-rich region of WAVE1 was amplified by PCR and subcloned in pGBT9 plasmid vector. This recombinant plasmid was transformed into Y190 yeast, which was then used as a host cell for screening. A human brain cDNA library (Clontech) was introduced into the transformed yeast and selected.

Recombinant proteins

We expressed various partial fragments of IRSp53 as GST–fusion forms in *Escherichia coli* using pGEX plasmids (Pharmacia). GST–fusion proteins of Grb2/Ash, Fyn, and p85 (phosphatidylinositol 3-kinase) were prepared as described[23]. Cdc42 and Rac were expressed as GST–fusion forms in Sf9 cells using recombinant baculoviruses, which were produced using the BAC-TO-BAC system (Gibco BRL). After purification with glutathione-sepharose beads, GST was cleaved off by thrombin treatment. Full-length WAVE1, WAVE2 and IRSp53 were also expressed as either GST–fusion forms or non-tagged forms in Sf9 cells by recombinant baculoviruses.

Antibodies

Rabbit polyclonal anti-WAVE antibody was prepared as described[10]. Anti-IRSp53 antibody was prepared in a rabbit immunized with the N-terminal 157-residue proteins expressed in *E. coli*. The antibody was affinity purified. We used commercially available antibodies for Myc-tag (polyclonal and monoclonal, both from Santa Cruz), Flag-tag (monoclonal from Sigma), Cdc42 (polyclonal from Santa Cruz), Rac (monoclonal from Transduction Laboratory) and GST (polyclonal from Santa Cruz). Control mouse IgG was purchased from Sigma.

Pull-down assay

GST–fusion proteins (10–50 µg) were first immobilized on 20 µl of glutathione-sepharose beads and then mixed with 400 µl protein samples such as cell lysates and purified proteins. After 2 h, the beads were washed with lysis buffer five times and 20 µl of SDS sample buffer was added. Samples (5 µl) were separated by SDS–PAGE, followed by immunoblotting and Coomassie staining. Cell lysates of Swiss3T3, COS7 and NIH3T3 cells were obtained by lysing half-confluent cells in a dish (diameter, 150 mm) with 1 ml lysis buffer. In the case of Sf9 cells infected with baculoviruses, cells were collected by centrifugation and then lysed in 1/20 volume of lysis buffer.

Ectopic expression in mammalian cells

NIH3T3 cells were transfected by the Ca^{2+}-phosphate method as described[23]. COS7 cells were transfected by electroporation as described[2]. In all expression analyses, pEF-BOS plasmid vectors[2] were used.

Pyrene actin assay

Actin was purified from rabbit muscle. We carried out pyrene labelling as described[9]. Arp2/3 complex was purified by affinity chromatography as described[5]. Arp2/3 complex and various proteins except actin were mixed in assay buffer (2 mM Tris-HCl (pH 8.0), 2 mM $MgCl_2$, 100 mM KCl, 0.2 mM $CaCl_2$, 0.2 mM ATP and 0.5 mM dithiothreitol). After incubation for 5 min at room temperature, actin (0.2 µM labelled actin in 2 µM non-labelled actin) was added and then subjected to fluorometry. Excitation and emission wavelengths were 365 nm and 407 nm, respectively.

1. Miki, H., Miura, K. & Takenawa, T. N-WASP, a novel actin-depolymerizing protein, regulates the cortical cytoskeletal rearrangement in a PIP2-dependent manner downstream of tyrosine kinases. *EMBO J.* **15**, 5326–5335 (1996).
2. Miki, H. *et al.* Induction of filopodium formation by a WASP-related actin-depolymerizing protein N-WASP. *Nature* **391**, 93–96 (1998).
3. Rozelle, A. L. *et al.* Phosphatidylinositol 4,5-bisphosphate induces actin-based movement of raft-enriched vesicles through WASP-Arp2/3. *Curr. Biol.* **10**, 311–320 (2000).
4. Suzuki, T. *et al.* Neural Wiskott–Aldrich syndrome protein is implicated in the actin-based motility of *Shigella flexneri*. *EMBO J.* **17**, 2767–2776 (1998).
5. Egile, C. *et al.* Activation of the CDC42 effector N-WASP by the *Shigella flexneri* IcsA protein promotes actin nucleation by Arp2/3 complex and bacterial actin-based motility. *J. Cell Biol.* **146**, 1319–1332 (1999).
6. Frischknecht, F. *et al.* Actin-based motility of vaccinia virus mimics receptor tyrosine kinase signalling. *Nature* **401**, 926–929 (1999).
7. Nobes, C. D. & Hall, A. Rho, rac, and cdc42 GTPases regulate the assembly of multimolecular focal complexes associated with actin stress fibers, lamellipodia, and filopodia. *Cell* **81**, 53–62 (1995).
8. Kozma, R. *et al.* The Ras-related protein Cdc42Hs and bradykinin promote formation of peripheral actin microspikes and filopodia in Swiss 3T3 fibroblasts. *Mol. Cell. Biol.* **15**, 1942–1952 (1995).
9. Rohatgi, R. *et al.* The interaction between N-WASP and the Arp2/3 complex links Cdc42-dependent signals to actin assembly. *Cell* **97**, 221–231 (1999).
10. Miki, H., Suetsugu, S. & Takenawa, T. WAVE, a novel WASP-family protein involved in actin reorganization induced by Rac. *EMBO J.* **17**, 6932–6941 (1998).
11. Ridley, A. J. *et al.* The small GTP-binding protein rac regulates growth factor-induced membrane ruffling. *Cell* **70**, 401–410 (1992).
12. Yeh, T. C. *et al.* Characterization and cloning of a 58/53-kDa substrate of the insulin receptor tyrosine kinase. *J. Biol. Chem.* **271**, 2921–2928 (1996).
13. Suetsugu, S., Miki, H. & Takenawa, T. Identification of two human WAVE/SCAR homologues as general actin regulatory molecules which associate with the Arp2/3 complex. *Biochem. Biophys. Res. Commun.* **260**, 296–302 (1999).
14. Bear, J. E., Rawls, J. F. & Saxe, C. L. III SCAR, a WASP-related protein, isolated as a suppressor of receptor defects in late *Dictyostelium* development. *J. Cell Biol.* **142**, 1325–1335 (1998).
15. Machesky, L. M. *et al.* Scar, a WASp-related protein, activates nucleation of actin filaments by the Arp2/3 complex. *Proc. Natl Acad. Sci. USA* **96**, 3739–3744 (1999).
16. Burbelo, P. D., Drechsel, D. & Hall, A. A conserved binding motif defines numerous candidate target proteins for both Cdc42 and Rac GTPases. *J. Biol. Chem.* **270**, 29071–29074 (1995).
17. Yarar, D. *et al.* The Wiskott–Aldrich syndrome protein directs actin-based motility by stimulating actin nucleation with the Arp2/3 complex. *Curr. Biol.* **9**, 555–558 (1999).
18. Mullins, R. D., Heuser, J. A. & Pollard, T. D. The interaction of Arp2/3 complex with actin: nucleation, high affinity pointed end capping, and formation of branching networks of filaments. *Proc. Natl Acad. Sci. USA* **95**, 6181–6186 (1998).
19. Blanchoin, L. *et al.* Direct observation of dendritic actin filament networks nucleated by Arp2/3 complex and WASP/Scar proteins. *Nature* **404**, 1007–1011 (2000).
20. Pantaloni, D. *et al.* The Arp2/3complex branches filament barbed ends functional antagonism with capping proteins. *Nature Cell Biol.* **2**, 385–391 (2000).
21. Bailly, M. *et al.* Relationship between Arp2/3 complex and the barbed ends of actin filaments at the leading edge of carcinoma cells after epidermal growth factor stimulation. *J. Cell Biol.* **145**, 331–345 (1999).
22. Svitkina, T. M. & Borisy, G. G. Arp2/3 complex and actin depolymerizing factor/cofilin in dendritic organization and treadmilling of actin filament array in lamellipodia. *J. Cell Biol.* **145**, 1009–1026 (1999).
23. Miki, H. *et al.* Phosphorylation of WAVE downstream of mitogen-activated protein kinase signaling. *J. Biol. Chem.* **274**, 27605–27609 (1999).

InsP$_4$ facilitates store-operated calcium influx by inhibition of InsP$_3$ 5-phosphatase

Meredith C. Hermosura*, **Hiroshi Takeuchi**†, **Andrea Fleig***, **Andrew M. Riley**‡, **Barry V. L. Potter**‡, **Masato Hirata**† **& Reinhold Penner***

* *Laboratory of Cell and Molecular Signaling, Center for Biomedical Research at The Queen's Medical Center and John A. Burns School of Medicine at The University of Hawaii, Honolulu, Hawaii 96813, USA*
† *Laboratory of Molecular and Cellular Biochemistry, Graduate School of Dental Sciences, Kyushu University and Kyushu University Station for Collaborative Research, Fukuoka 812-8582, Japan*
‡ *Wolfson Laboratory of Medicinal Chemistry, Department of Pharmacy & Pharmacology, University of Bath, Claverton Down, Bath BA2 7AY, UK*

Receptor-mediated generation of inositol 1,4,5-trisphosphate (InsP$_3$) initiates Ca^{2+} release from intracellular stores and the subsequent activation of store-operated calcium influx[1]. InsP$_3$ is metabolized within seconds by 5-phosphatase and 3-kinase[2], yielding Ins(1,4)P$_2$ and inositol 1,3,4,5-tetrakisphosphate (InsP$_4$), respectively. Some studies have suggested that InsP$_4$ controls Ca^{2+} influx in combination with InsP$_3$ (refs 3 and 4), but another study did not find the same result[5]. Some of the apparent conflicts between these previous studies have been resolved[6]; however, the physiological function of InsP$_4$ remains elusive[7,8]. Here we have investigated the function of InsP$_4$ in Ca^{2+} influx in the mast cell line RBL-2H3, and we show that InsP$_4$ inhibits InsP$_3$ metabolism through InsP$_3$ 5-phosphatase, thereby facilitating the activation of the store-operated Ca^{2+} current I_{CRAC} (ref. 9). Physiologically, this mechanism opens a discriminatory time window for coincidence detection that enables selective facilitation of Ca^{2+} influx by appropriately timed low-level receptor stimulation. At higher

concentrations, $InsP_4$ acts as an inhibitor of $InsP_3$ receptors, enabling $InsP_4$ to act as a potent bi-modal regulator of cellular sensitivity to $InsP_3$, which provides both facilitatory and inhibitory feedback on Ca^{2+} signalling.

Evidence suggests that a functionally distinct store is involved in activating I_{CRAC} and that depletion of this store requires fairly high $InsP_3$ levels[10,11]. This lower $InsP_3$ sensitivity is probably due to $InsP_3$ metabolism through 5-phosphatase, which results in a nonlinear relationship between $InsP_3$ concentration and I_{CRAC} activation[10,12]. As early work on 5-phosphatase identified $InsP_4$ as an inhibitor of this enzyme *in vitro*[2], we performed whole-cell patch-clamp experiments in which we perfused $InsP_4$ and other potential 5-phosphatase inhibitors in combination with $InsP_3$. We found that inhibition of 5-phosphatase-dependent $InsP_3$ metabolism facilitates activation of I_{CRAC}.

Perfusion of 20 μM $InsP_4$ into RBL-2H3-M1 cells, a transfected cell line that stably expresses muscarinic M1 receptors[13], produces no measurable Ca^{2+} release nor does it activate Ca^{2+} influx ($n = 12$; Fig. 1a). By contrast, carbachol-stimulated production of $InsP_3$ causes a sharp Ca^{2+} release transient followed by activation of store-operated Ca^{2+} entry. This carbachol-stimulated Ca^{2+} influx accounts for the Ca^{2+} increases during hyperpolarizing shifts in membrane potential. Similarly, under experimental conditions that favour electrophysiological detection of the store-operated Ca^{2+} current I_{CRAC} (ref. 9), $InsP_4$ (20 μM, $n = 12$) failed to activate

I_{CRAC}, whereas the same concentration of $InsP_3$ readily did so ($n = 36$; Fig. 1b).

We next assessed the effects of $InsP_4$ on I_{CRAC} in combination with defined $InsP_3$ concentrations. Activation of I_{CRAC} occurs over a concentration range of 2 to 5 μM (Fig. 1d; see also ref. 10); however, in the presence of $InsP_4$ the threshold for $InsP_3$-mediated activation of I_{CRAC} is lowered considerably, enabling cells to develop the current even at subthreshold $InsP_3$ levels (1 μM and less). $InsP_3$ at concentrations of 2–5 μM activates I_{CRAC} with near-maximal amplitude, but with a delay and slow-activation time constant (Fig. 1d). At these $InsP_3$ concentrations, $InsP_4$ facilitates activation of I_{CRAC} by reducing the delay and by speeding-up activation of the current. Facilitation by $InsP_4$, however, is no longer evident at high, saturating $InsP_3$ concentrations (above 5 μM; Figs 1d and 2a). As $InsP_4$ is produced in numerous cell types, we tested whether the facilitation of I_{CRAC} also occurs in Jurkat T lymphocytes, another immune cell line with store-operated currents that are well characterized[14]. $InsP_4$ also facilitates I_{CRAC} activation induced by 1 μM $InsP_3$ in T cells (Fig. 1c), indicating that this mechanism may be of general importance.

The effects of $InsP_4$ on $InsP_3$-mediated I_{CRAC} activation are shown in Fig. 2. First, $InsP_4$ lowers the threshold at which $InsP_3$ activates I_{CRAC}, which results in a significant left shift ($P < 0.05$) of the $InsP_3$ dose–response curve (Fig. 2a). Second, $InsP_4$ reduces delays in activation of the current, particularly at threshold levels (2–3 μM)
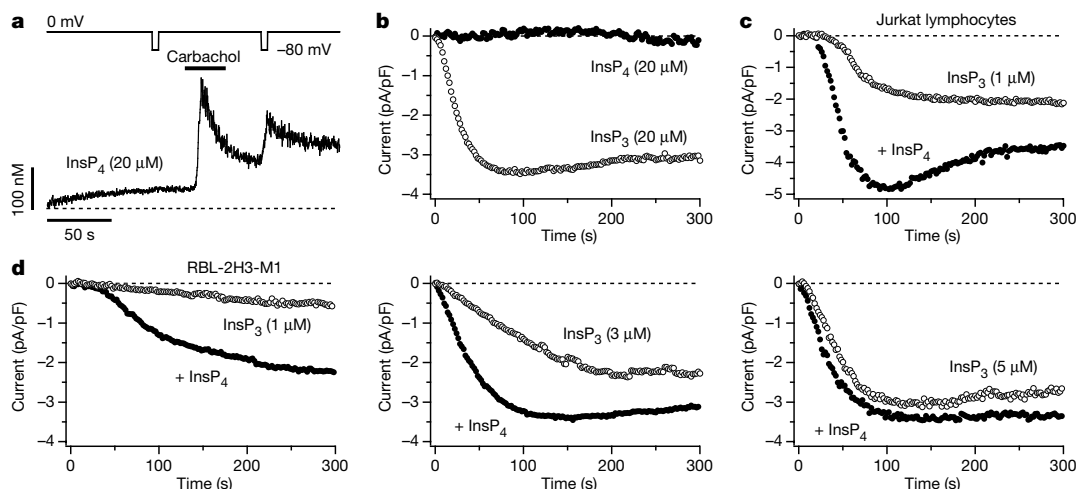
Figure 1 $InsP_4$ facilitates $InsP_3$-dependent activation of I_{CRAC}. **a**, Representative $[Ca^{2+}]_i$ measurement in a patch-clamped RBL-2H3-M1 cell perfused with 20 μM $InsP_4$. Identical hyperpolarizations to −80 mV (top trace) were induced before and after carbachol (100 μM) challenge to increase the driving force for Ca^{2+} and probe Ca^{2+} entry. **b**, Average inward currents of RBL-2H3-M1 cells at −80 mV in the presence of 20 μM $InsP_4$ ($n = 12$) and 20 μM $InsP_3$ ($n = 36$). **c**, Average inward currents at −80 mV of Jurkat

lymphocytes perfused with 1 μM $InsP_3$ ($n = 6$) or in combination with 20 μM $InsP_4$ ($n = 6$). **d**, Average inward currents of RBL-2H3-M1 cells at −80 mV in response to a given $InsP_3$ concentration or in combination with 20 μM $InsP_4$. Experimental conditions in **b**–**d** are optimized for electrophysiological detection of I_{CRAC} (10 mM external Ca^{2+} and $[Ca^{2+}]_i$ buffered to 100 nM by 10 mM BAPTA + 4.3 mM $CaCl_2$).
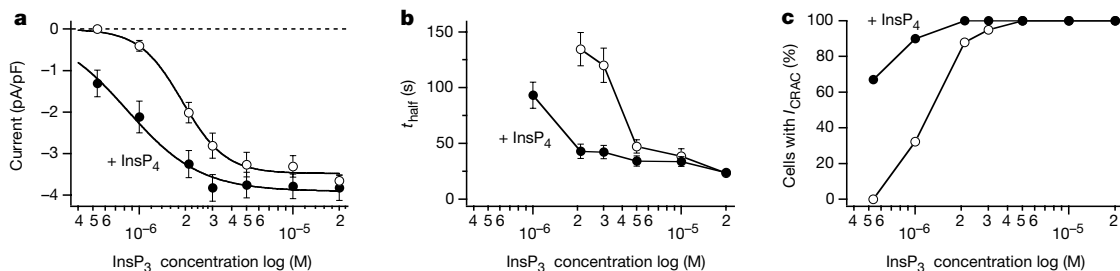
Figure 2 Quantitative analysis of $InsP_4$-induced facilitation of I_{CRAC}. **a**, Average peak amplitude of I_{CRAC} (± s.e.m., $n = 14$–35) at −80 mV induced by concentrations of $InsP_3$ and by the additional presence of 20 μM $InsP_4$. Half-maximal effective concentration (EC_50) required for I_{CRAC} activation is 1.9 μM for $InsP_3$ and 830 nM for $InsP_3 + InsP_4$. The difference between the data sets is highly significant ($P = 0.007$, paired t-test). **b**, Average

time required for half-maximal activation of I_{CRAC} (t_{half} ± s.em., $n = 14$–35). Student's t-test evaluates the differences for data obtained at 2 μM and 3 μM $InsP_3$ as highly significant at $P = 0.000003$ and $P = 0.000002$, respectively. At 5 μM and 10 μM $InsP_3$, the difference becomes insignificant with $P = 0.09$ and $P = 0.56$, respectively. **c**, Percentage of cells that develop I_{CRAC}.

of InsP$_3$ (Fig. 2b). Last, InsP$_4$ increases the percentage of cells that activate I_{CRAC} at low InsP$_3$ concentrations (Fig. 2c) so that, in the presence of InsP$_4$, a dose as low as 2 μM InsP$_3$ can evoke I_{CRAC} in 100% of the cells tested, whereas at least 5 μM InsP$_3$ is needed to obtain this level of I_{CRAC} activation when only InsP$_3$ is used. Thus, InsP$_4$ is particularly effective at low InsP$_3$ concentrations (0.5– 3 μM), where it mediates statistically significant facilitation of I_{CRAC} activation ($P < 0.05$).

As InsP$_4$ can also be metabolized, albeit to a lesser extent than can InsP$_3$, we investigated whether downstream metabolites of InsP$_3$ or InsP$_4$ could account for the observed stimulatory effects on I_{CRAC}. However, none of the various inositol phosphates that lack intrinsic Ca^{2+} release activity was effective in facilitating activation of I_{CRAC} at concentrations of 1–40 μM (data not shown). In addition, the inability of InsP$_4$ to induce either Ca^{2+} release or activation of I_{CRAC} (Fig. 1) eliminates the possibility that it produces inositol phosphates with release activity, such as InsP$_3$ or Ins(1,4,6)P$_3$ (ref. 15). Furthermore, other possible direct actions of InsP$_4$ do not seem to be involved in this particular aspect of InsP$_4$ function, as InsP$_4$ does not lead to activation of I_{CRAC} and seems to enhance Ca^{2+} influx only when combined with InsP$_3$.

These data suggested that other InsP$_3$ 5-phosphatase inhibitors should behave in a similar way to InsP$_4$. To test this hypothesis directly, we studied three analogues that are inhibitory to InsP$_3$ 5-phosphatase (see Fig. 3a for structures): L-*myo*-inositol 1,3,4,5-tetra-kisphosphate, (L-InsP$_4$); the enantiomer of InsP$_4$, L-threitol-1,2,4-trisphosphate (L-Thre(1,2,4)P$_3$); and D-2,3-bisphosphoglycerate (D-2,3-PG), which acts as a competitive inhibitor of 5-phosphatase[16]. We synthesized L-Thre(1,2,4)P$_3$ specifically to

improve the inhibitory actions of D-2,3-PG, whereas L-InsP$_4$ was expected to have inhibitory effects on the basis of its structural similarity to InsP$_4$. We confirmed that D-InsP$_4$, as well as the above compounds, inhibits 5-phosphatase by acting as a co-substrate (Fig. 3b). D-InsP$_4$ is the most potent 5-phosphatase inhibitor, (IC$_{50}$ (half-maximal inhibitory concentration) ≈ 0.15 μM) and is at least one order of magnitude more effective than L-InsP$_4$, (IC$_{50}$ ≈ 1.8 μM). The physiological metabolite D-InsP$_4$ seems to be more potent than previously described synthetic 5-phosphatase inhibitors[17], such as L-*chiro*-Ins(2,3,5)PS$_3$ (IC$_{50}$ ≈ 0.23 μM) and L-*chiro*-Ins(1,4,6)PS$_3$ (IC$_{50}$ ≈ 0.30 μM).

Figure 3e shows the average inward currents of cells perfused with the threshold concentration of 1 μM InsP$_3$ and each of the inhibitors. Three of the 5-phosphatase inhibitors facilitated InsP$_3$-mediated activation of I_{CRAC}, with D-InsP$_4$ being the most effective, followed by L-Thre(1,2,4)P$_3$ and then D-2,3-PG (see also Table 1). Notably, L-InsP$_4$ was completely ineffective in facilitating I_{CRAC}, although it is a potent inhibitor of 5-phosphatase, second only to D-InsP$_4$ (Fig. 3b).

As D-2,3-PG interacts with InsP$_3$ receptors[16], we looked at the potential interaction of 5-phosphatase inhibitors with InsP$_3$ receptors (InsP$_3$R). InsP$_3$ binding assays show that all four compounds inhibit InsP$_3$-binding to InsP$_3$R with an order of potency similar to that of 5-phosphatase inhibition (Fig. 3c). InsP$_3$R binding and 5-phosphatase inhibition would have opposing effects on InsP$_3$-mediated activation of I_{CRAC}, with the first contributing a positive effect and the second contributing a negative effect. The resulting net-facilitation curves (Fig. 3d) can be calculated as the product of these two factors, where the amplitude reflects efficacy and the location of the curve on the x axis reflects potency. These net-facilitation curves predict InsP$_4$ to be the most potent and the most effective facilitator of I_{CRAC} activation, followed by L-Thre(1,2,4)P$_3$ and then D-2,3-PG. L-InsP$_4$ is predicted to be the least effective, because its strong inhibition of InsP$_3$ binding essentially obliterates any facilitation through 5-phosphatase.

These predictions are confirmed qualitatively by patch-clamp experiments, which clearly show that InsP$_4$ provides the most effective facilitation of I_{CRAC}, whereas its enantiomer, L-InsP$_4$, has no measurable effect (Fig. 3e and Table 1). D-2,3-PG and L-Thre(1,2,4)P$_3$ are similar both in efficacy and in delay of activation (Table 1). Although a high efficacy (y axis) of D-2,3-PG is predicted in Fig. 3d, the potency of D-2,3-PG (x axis) peaks at fairly high concentrations above 100 μM; however, there is maximum enhancement of I_{CRAC} activation with 10–20 μM D-2,3-PG, with decreasing effects above 100 μM. Similarly, the net-facilitation curve for InsP$_4$ predicts it to be most potent at about 100 nM to 1 μM, but there is no facilitation until 5 μM. Although the biochemical data are in good agreement with the rank order of efficacy
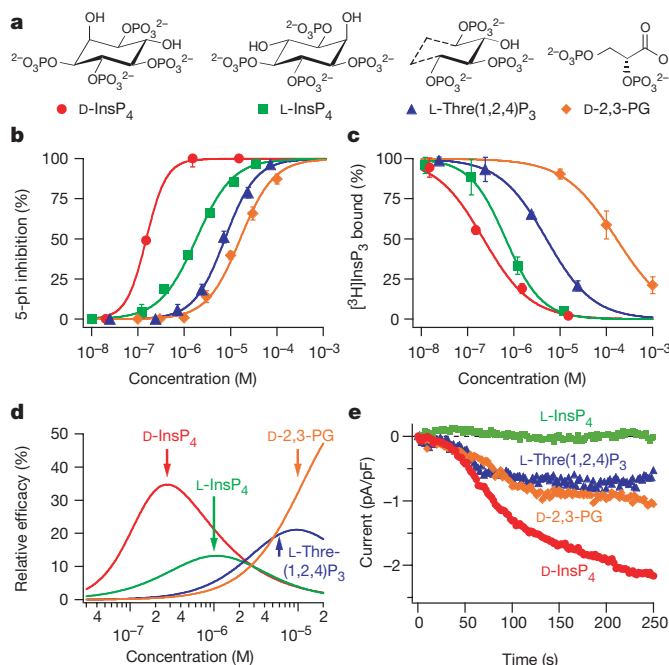
Figure 3 InsP$_4$ and related compounds inhibit 5-phosphatase and InsP$_3$ receptor binding. **a**, Chemical structures of 5-phosphatase inhibitors. L-InsP$_4$ is shown in a binding orientation in which it can mimic its enantiomer D-InsP$_4$; the relationship of the acyclic L-Thre(1,2,4)P$_3$ to InsP$_3$ / InsP$_4$ is shown by a dashed line. **b**, Inhibition profile of type I 5-phosphatase activity (see Methods). Data points are averages ± s.e.m. ($n = 3$). **c**, Inhibition profile of [^{3}H] InsP$_3$ binding to InsP$_3$ receptors (see Methods). Data points are averages ± s.e.m. ($n = 3$). **d**, Facilitation profiles of 5-phosphatase inhibitors. Net-facilitation curves reflect the product of inhibition profiles of 5-phosphatase activity and InsP$_3$ binding of InsP$_3$ receptors from **b** and **c**. **e**, Average inward currents carried by I_{CRAC} at −80 mV. Cells are co-perfused with various 5-phosphatase inhibitors and subthreshold levels of InsP$_3$ (1 μM). Traces are averages of experiments in which D-InsP$_4$ ($n = 14$), L-InsP$_4$ ($n = 15$) and L-Thre(1,2,4)P$_3$ ($n = 5$) were used at 20 μM. D-2,3-PG ($n = 4$) was used at 10 μM.

Table 1 5-Phosphatase inhibitors facilitate Ins(1,4,5)P$_3$-mediated activation of I_{CRAC}

	D-InsP$_4$	L-Thre(1,2,4)P$_3$	D-2,3-PG	L-InsP$_4$
Peak current (pA/pF)*	−2.1 ± 0.4	−1.1 ± 0.3	−0.9 ± 0.4	0
	($n = 14$)	($n = 5$)	($n = 4$)	($n = 15$)
Half-maximal activation (s)*	93 ± 12	71 ± 14	79 ± 9	n.a.
	($n = 14$)	($n = 5$)	($n = 4$)	
Concentrations tested (μM)	1–20	10–100	10–1,000	1–50
Most effective concentration (μM)	5–20	100	10–20	n.a.
IC$_{50}$ for 5-phosphatase (μM)†	0.15	7.5	16.0	1.8
IC$_{50}$ for [^{3}H]Ins(1,4,5)P$_3$ binding (μM)†	0.22	5.0	165	0.66

* Values of peak currents and half-maximal activation times of I_{CRAC} represent means ± s.e.m. They are derived from time course analysis of inward currents illustrated in Fig. 3e and correspond to experiments in which inhibitors were used at 20 μM, except D-2,3-PG, which was used at 10 μM.
† Half-maximal inhibitory concentrations (IC$_{50}$) for 5-phosphatase and Ins(1,4,5)P$_3$ binding are derived from dose–response fits to data sets presented in Fig. 3b and c, respectively. n.a., not applicable.
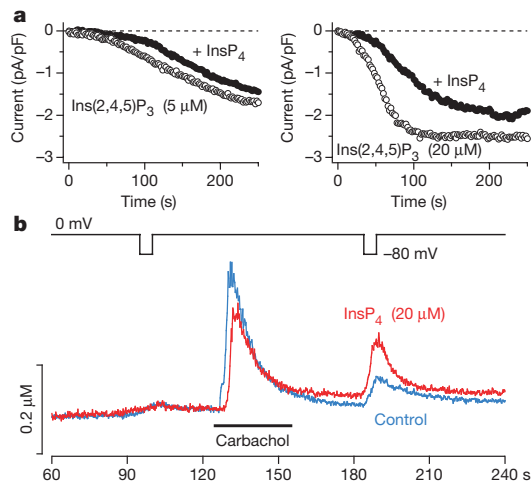
of the test compounds in facilitating I_{CRAC}, it seems that the potencies cannot be predicted accurately, simply from the combined effects of 5-phosphatase inhibition and InsP$_3$R binding. This is not an unexpected conclusion as the predictions are based on *in vitro* biochemical analyses, which do not necessarily replicate *in vivo* conditions. In addition, the InsP$_3$-binding data were obtained from cerebellar microsomes, which contain mainly type I InsP$_3$ receptors[18], whereas RBL cells have a mixed set of InsP$_3$ receptors[19], primarily comprising of type II. Possibly, interaction of InsP$_4$ and the other analogues with InsP$_3$ receptors may be subtype-specific,

Figure 4 InsP$_4$ does not facilitate non-metabolizable Ins(2,4,5)P$_3$. **a**, Left, average inward currents carried by I_{CRAC} at −80 mV induced by 5 μM Ins(2,4,5)P$_3$ alone ($n = 8$) and by 5 μM Ins(2,4,5)P$_3$ + 20 μM InsP$_4$ ($n = 8$). Right, average inward currents induced by 20 μM Ins(2,4,5)P$_3$ ($n = 8$) and by 20 μM Ins(2,4,5)P$_3$ + 20 μM InsP$_4$ ($n = 7$). **b**, Average [Ca^{2+}]$_i$ signals in patch-clamped RBL-2H3-M1 cells. Blue control trace shows cells perfused with standard internal solution ($n = 10$); red trace shows responses of cells perfused with 20 μM InsP$_4$ ($n = 8$). Identical hyperpolarizations to −80 mV were induced before and after carbachol (100 μM) challenge to increase the driving force for Ca^{2+} and probe the magnitude of Ca^{2+} entry.

just as the sensitivities of InsP$_3$ receptor subtypes to InsP$_3$ are different[15].

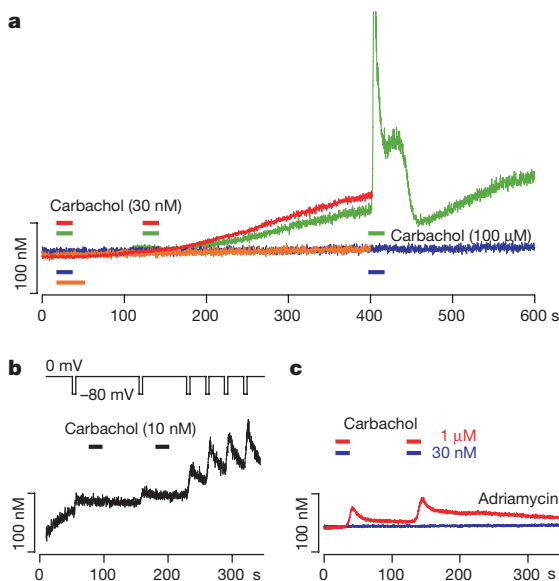If InsP$_4$ acts primarily by regulating InsP$_3$ metabolism, then InsP$_4$ should be largely ineffective when I_{CRAC} is activated by Ins(2,4,5)P$_3$, a non-metabolizable analogue of InsP$_3$. This is confirmed in Fig. 4a, which shows development of I_{CRAC} in cells perfused with InsP$_4$ and 5 μM or 20 μM Ins(2,4,5)P$_3$. InsP$_4$ does not facilitate Ins(2,4,5)P$_3$-mediated activation of I_{CRAC}, but instead inhibits it; a finding that is compatible with the inhibition of Ca^{2+} influx observed in lacrimal cells[20] and presumably stems from the competitive antagonism of InsP$_4$ on InsP$_3$ receptors (Fig. 3c). Therefore, InsP$_4$ can compete effectively with Ins(2,4,5)P$_3$ for the InsP$_3$ receptors, but cannot influence Ins(2,4,5)P$_3$ levels as they are not regulated by 5-phosphatase.

We next tested for effects of InsP$_4$ on Ca^{2+} signals induced by receptor stimulation. Figure 4b shows carbachol-induced Ca^{2+} signals in RBL-2H3-M1 cells in the presence (5−20 μM InsP$_4$; $n = 13$) and absence of InsP$_4$. Carbachol application induces Ca^{2+} release, and the time to peak of the release transient in the presence of InsP$_4$ occurs with a statistically significant delay of 4 s (control, 4.2 ± 0.3 s; + InsP$_4$, 8.6 ± 0.9 s, $P = 0.0008$). No statistical significance was found for maximal release rates (control, 237 ± 38 nM s^{-1}; + InsP$_4$, 155 ± 28 nM s^{-1}, $P = 0.09$). This is consistent with a competitive antagonism of InsP$_4$ on InsP$_3$ receptors. After Ca^{2+} release, Ca^{2+} influx is activated and, unlike the first hyperpolarization, the second one triggers a change in [Ca^{2+}]$_i$, which, in the presence of InsP$_4$, is larger and more sustained than that of control cells. Analysis of control and InsP$_4$-enhanced influx phases, by integrating the area under the influx transient (10 s period), reveals statistically significant enhancement of Ca^{2+} entry that leads to a twofold increase in [Ca^{2+}]$_i$ (control, 441 ± 81 nM s^{-1}; + InsP$_4$, 858 ± 109 nM s^{-1}; $P = 0.008$).

In intact cells, InsP$_4$ is produced by InsP$_3$ 3-kinases[21] at the expense of InsP$_3$ itself. Nevertheless, InsP$_4$ could ultimately induce a net elevation of InsP$_3$ levels where metabolism through 5-phosphatase outweighs that of the 3-kinase, for example, underneath the plasma membrane where 5-phosphatase is localized[22]. Therefore, low levels of InsP$_3$ generated by an initial weak-agonist signal may

Figure 5 InsP$_4$ selectively facilitates Ca^{2+} influx. **a**, Average intracellular Ca^{2+} signals in intact RBL-2H3-M1 cells stimulated by low levels of carbachol. Two identical carbachol stimuli (30 nM) of 15-s duration were delivered at intervals of 0 s (orange trace, $n = 7$), 90 s (red trace, $n = 20$) and 365 s (blue trace, $n = 6$). The green trace (shifted down by 5 nM for illustration purposes) represents a subset of 6 cells of the 20 red trace cells that were stimulated a third time by 100 μM carbachol in Ca^{2+}-free solution. **b**, Average

intracellular Ca^{2+} signals ($n = 3$) of cells perfused with standard internal solution and stimulated as in **a**. **c**, Average intracellular Ca^{2+} signals in intact RBL-2H3-M1 cells stimulated by subthreshold (30 nM, $n = 14$) and threshold (1 μM, $n = 6$) levels of carbachol. Stimulation of cells was performed as in **a** after pre-incubation with adriamycin (10 μM) for 2 h. The red trace was shifted up by 10 nM for display purposes.

738 NATURE | VOL 408 | 7 DECEMBER 2000 | www.nature.com

induce spatially confined InsP$_3$ production that, owing to effective metabolism, is not sufficient to cause Ca^{2+} release or to activate I_{CRAC}. However, the concomitant production of InsP$_4$ might prime and sensitize cells to respond more effectively to a second stimulation by the same, or different agonist. We challenged receptor-mediated Ca^{2+} signals in intact RBL-2H3-M1 cells with two identical stimuli of 30 nM carbachol, which were delivered for 15 s at different time intervals (Fig. 5a). This agonist concentration is well below the threshold for measurable Ca^{2+} release, and we observed no visible Ca^{2+} signal after the first stimulus. Continued stimulation for another 15 s also failed to induce a Ca^{2+} signal (Fig. 5a; orange trace). However, when the second identical stimulus was given after 90 s, 20 out of 24 cells generated a long-lasting plateau of elevated [Ca^{2+}]$_i$ (Fig. 5a, red trace). Such facilitation was not observed when the second carbachol application was delivered with a delay of 365 s (Fig. 5a, blue trace).

These results suggest that the first carbachol stimulation generates a priming factor that facilitates subsequent Ca^{2+} signalling. In RBL-2H3-M1 cells, carbachol only produces diacylglycerol and InsP$_3$. As diacylglycerol activates protein kinase C, which is known to cause inhibition of Ca^{2+} influx in RBL cells[23], we must conclude that the facilitation is due to an inositol phosphate, specifically InsP$_4$, as its lifetime is consistent with the time window of facilitation[24] and all other inositol phosphates failed to facilitate I_{CRAC} (data not shown). The results also suggest that a local increase in InsP$_3$ levels can selectively release Ca^{2+} from stores that activate I_{CRAC} ('CRAC stores'). As Ca^{2+} release from these 'CRAC stores' does not contribute significantly to global cytosolic Ca^{2+} signals[10], there is only a Ca^{2+} influx signal and no visible Ca^{2+} transient. The experiments shown by the green trace in Fig. 5a support this idea. There the facilitation of Ca^{2+} signalling proceeds as in the red trace; a subsequent challenge with a large dose of carbachol (100 μM) releases all Ca^{2+} from InsP$_3$-sensitive stores, which results in a large Ca^{2+} release transient. Thus, it seems that 'CRAC stores' can be emptied by localized InsP$_3$ signalling, whereas the bulk of InsP$_3$-sensitive stores remain full.

The experiments in intact cells were done in Cs$^+$-containing external solution, which minimizes agonist-mediated changes in membrane potential that could indirectly enhance Ca^{2+} influx. To further exclude any such effect and to ascertain that the Ca^{2+} signal facilitation was due to Ca^{2+} influx, we confirmed that facilitation of a second subthreshold carbachol stimulus also occurs when stimulating cells in the whole-cell configuration (Fig. 5b). As in the intact cells, carbachol did not induce Ca^{2+} release, but selectively facilitated Ca^{2+} influx, as changes in [Ca^{2+}]$_i$ during membrane hyperpolarizations were significantly enhanced after the second, but not the first, application of carbachol.

We also tested adriamycin (doxorubicin), which is known to inhibit InsP$_3$ 3-kinase[25] and suppress InsP$_4$ production. Cells treated with 10 μM adriamycin did not have a facilitated Ca^{2+} influx component after a second subthreshold carbachol stimulation (Fig. 5c, blue trace). Adriamycin also suppressed facilitation in patch-clamped cells and did not inhibit I_{CRAC} directly (data not shown), thereby eliminating nonspecific drug effects on ion channels. We can also eliminate reduced InsP$_3$ production as a possible side-effect, as the threshold carbachol concentration of 1 μM in adriamycin-treated cells was similar to that of control RBL cells and produced enough InsP$_3$ to consistently reach the threshold for visible Ca^{2+} release (Fig. 5c, red trace). Even under these conditions, adriamycin largely suppressed the facilitatory effects on Ca^{2+} signalling. Therefore, the adriamycin experiments are consistent with the hypothesis that InsP$_4$ production mediated by InsP$_3$ 3-kinase is primarily responsible for the observed facilitation of repetitive subthreshold stimuli.

We have presented evidence that shows InsP$_4$ to be a potent, naturally occurring 5-phosphatase inhibitor that facilitates Ca^{2+} influx by sensitizing InsP$_3$-mediated activation of I_{CRAC}. As InsP$_4$ production occurs at the expense of InsP$_3$, and high levels of InsP$_4$ can inhibit InsP$_3$ receptors, it is possible that in some cell systems, the overall effect of InsP$_4$ on Ca^{2+} signalling may be inhibitory. This would apply particularly to cells with high levels of endogenous or experimentally over-expressed InsP$_3$ 3-kinase[22,26]. The impact of InsP$_4$ on Ca^{2+} signalling may be multifaceted and cell-type specific, varying with strength of receptor stimulation, subcellular localization of InsP$_3$-metabolizing enzymes, heterogeneity of intracellular Ca^{2+} stores, InsP$_3$ receptor subtype composition and additional regulatory mechanisms that affect the above. □

Methods

Synthetic inositol phosphates and 5-phosphatase inhibitors

We synthesized D-InsP$_4$ and L-InsP$_4$ as described[27]. L-Thre(1,2,4)P$_3$ was prepared from (2S,3S)-(+)-2-benzyloxybutane-1,3,4-triol (Fluka). Briefly, phosphitylation of the triol with N,N-diethyl-1,5-dihydro-2,4,3-benzodioxaphosphepin-3-amine in the presence of 1H-tetrazole, followed by oxidation in situ with 3-chloroperoxybenzoic acid, gave the protected trisphosphate, which was purified by flash chromatography on silica gel. Deprotection by hydrogenolysis over palladium on carbon gave L-Thre(1,2,4)P$_3$, which was purified by ion-exchange chromatography on Q-Sepharose fast flow resin before use. All synthetic compounds showed analytical and spectroscopic data in full accordance with structure. We obtained other inositol phosphates and D-2,3-PG from Sigma.

5-Phosphatase inhibition and InsP$_3$ receptor-binding assays

The assays of InsP$_3$ 5-phosphatase activity were performed at pH 7.2 using purified recombinant enzyme expressed in Escherichia coli as described[28]. We performed the InsP$_3$ receptor-binding assays by using microsomal fractions of rat cerebellum prepared as described[29]. The assay mixture (0.5 ml) contained 50 mM HEPES/NaOH buffer pH 7.2, 1 mM EDTA, 6 nM [3H] InsP$_3$ and ~30 μg of microsomal fraction, in the presence of various concentrations of compounds of interest. Incubation was performed on ice for 10 min, followed by the separation of bound radioactivity from free form by centrifugation (15,000 r.p.m. for 10 min). Nonspecific binding (150–200 d.p.m.) was determined in the presence of 10 μM InsP$_3$ and was subtracted from that in its absence to determine the specific binding (4,000–5,000 d.p.m.).

Electrophysiology

For patch-clamp experiments, RBL-2H3-M1 cells grown on glass coverslips were transferred to the recording chamber and kept in a standard modified Ringer's solution containing (in mM): 145 NaCl, 2.8 KCl, 10 CsCl, 10 CaCl$_2$, 2 MgCl$_2$, 10 glucose, 10 HEPES NaOH, pH 7.2. We used CsCl to inhibit inward rectifier potassium currents. For Ca^{2+} measurements, the external Ca^{2+} concentration was adjusted to 2 mM. We used carbachol at the indicated concentrations. The standard intracellular pipette-filling solution contained (in mM): 145 caesium-glutamate, 8 NaCl, 1 MgCl$_2$, 0.5 Mg-ATP, 0.3 GTP, pH 7.2, adjusted with CsOH. Except for the fura-2 experiments, the internal solution was supplemented with a mixture of 10 mM caesium-BAPTA and 4.3–5.3 mM CaCl$_2$ to buffer [Ca^{2+}]$_i$ to resting levels of 100–150 nM and to avoid spontaneous activation of I_{CRAC}. We carried out patch-clamp experiments in the tight-seal whole-cell configuration at 21–25 °C. We acquired high-resolution current recordings by a computer-based patch-clamp amplifier system (EPC-9, HEKA, Lambrecht, Germany). Patch pipettes had resistances between 2 and 4 MΩ after filling with the standard intracellular solution. Immediately after establishment of the whole-cell configuration, voltage ramps of 50-ms duration spanning the voltage range of −100 to +100 mV were delivered from a holding potential of 0 mV at a rate of 0.5 Hz over a period of 300–400 s. All voltages were corrected for a liquid junction potential of 10 mV between external and internal solutions. We filtered currents at 2.3 kHz and digitized them at 100-μs intervals. Capacitive currents and series resistance were determined and corrected before each voltage ramp using the automatic capacitance compensation of the EPC-9. For analysis, the very first ramps before activation of I_{CRAC} (usually 1–3) were digitally filtered at 2 kHz, pooled and used for leak subtraction of all subsequent current records. The low-resolution temporal development of inward currents was extracted from the leak-corrected individual ramp current records by measuring the current amplitude at −80 mV.

Calcium measurements

The cytosolic calcium concentration of individual patch-clamped or intact cells was monitored at a rate of 5 Hz with a photomultiplier-based system using a monochromatic light source tuned to excite fura-2 fluorescence at 360 and at 390 nm for 20 ms each. Emission was detected at 450–550 nm with a photomultiplier whose analogue signals were sampled and processed by the X-Chart software package (HEKA, Lambrecht, Germany). Fluorescence ratios were translated into free intracellular calcium concentration on the basis of calibration parameters derived from patch-clamp experiments with calibrated calcium concentrations. In patch-clamp experiments, we added fura-2 to the standard intracellular solution at 100 μM. Ester loading of intact cells was performed by incubating cells for 45–60 min in standard solution (2 mM extracellular calcium) supplemented with 5 μM fura-2-AM. In all experiments, where intracellular Ca^{2+} was monitored (patch-clamp or intact cells), the standard external solution contained 2 mM Ca^{2+}. Local perfusion of individual cells with carbachol was achieved through a wide-tipped, pressure-controlled application pipette (3 μm diameter) placed approximately 30 μm from the cell under investigation.

letters to nature

1. Parekh, A. B. & Penner, R. Store depletion and calcium influx. *Physiol. Rev.* **77**, 901–930 (1997).
2. Connolly, T. M., Bansal, V. S., Bross, T. E., Irvine, R. F. & Majerus, P. W. The metabolism of tris- and tetraphosphates of inositol by 5-phosphomonoesterase and 3-kinase enzymes. *J. Biol. Chem.* **262**, 2146–2149 (1987).
3. Irvine, R. F. & Moor, R. M. Micro-injection of inositol 1,3,4,5-tetrakisphosphate activates sea urchin eggs by a mechanism dependent on external Ca^{2+}. *Biochem. J.* **240**, 917–920 (1986).
4. Morris, A. P., Gallacher, D. V., Irvine, R. F. & Petersen, O. H. Synergism of inositol trisphosphate and tetrakisphosphate in activating Ca^{2+}-dependent K$^+$ channels. *Nature* **330**, 653–655 (1987).
5. Bird, G. S. *et al.* Activation of Ca^{2+} entry into acinar cells by a non-phosphorylatable inositol trisphosphate. *Nature* **352**, 162–165 (1991).
6. Smith, P. M., Harmer, A. R., Letcher, A. J. & Irvine, R. F. The effect of inositol 1,3,4,5-tetrakisphosphate on inositol trisphosphate-induced Ca^{2+} mobilization in freshly isolated and cultured mouse lacrimal acinar cells. *Biochem. J.* **347**, 77–82 (2000).
7. Fukuda, M. & Mikoshiba, K. The function of inositol high polyphosphate binding proteins. *BioEssays* **19**, 593–603 (1997).
8. Cullen, P. J. Bridging the GAP in inositol 1,3,4,5-tetrakisphosphate signalling. *Biochim. Biophys. Acta* **1436**, 35–47 (1998).
9. Hoth, M. & Penner, R. Depletion of intracellular calcium stores activates a calcium current in mast cells. *Nature* **355**, 353–356 (1992).
10. Parekh, A. B., Fleig, A. & Penner, R. The store-operated calcium current I_{CRAC}: nonlinear activation by InsP$_3$ and dissociation from calcium release. *Cell* **89**, 973–980 (1997).
11. Broad, L. M., Armstrong, D. L. & Putney, J. W. Role of the inositol 1,4,5-trisphosphate receptor in Ca^{2+} feedback Inhibition of calcium release-activated calcium current I_{CRAC}. *J. Biol. Chem.* **274**, 32881–32888 (1999).
12. Glitsch, M. D. & Parekh, A. B. Ca^{2+} store dynamics determines the pattern of activation of the store-operated Ca^{2+} current I_{CRAC} in response to InsP$_3$ in rat basophilic leukaemia cells. *J. Physiol. (Lond.)* **523**, 283–290 (2000).
13. Jones, S. V., Choi, O. H. & Beaven, M. A. Carbachol induces secretion in a mast cell line (RBL-2H3) transfected with the M1 muscarinic receptor gene. *FEBS Lett.* **289**, 47–50 (1991).
14. Lewis, R. S. & Cahalan, M. D. Potassium and calcium channels in lymphocytes. *Annu. Rev. Immunol.* **13**, 623–653 (1995).
15. Hirata, M. *et al.* Inositol 1,4,5-trisphosphate receptor subtypes differentially recognize regioisomers of D-*myo*-inositol 1,4,5-trisphosphate. *Biochem. J.* **328**, 93–98 (1997).
16. Guillemette, G., Favreau, I., Lamontagne, S. & Boulay, G. 2,3-Diphosphoglycerate is a nonselective inhibitor of inositol 1,4,5-trisphosphate action and metabolism. *Eur. J. Pharmacol.* **188**, 251–260 (1990).
17. Safrany, S. T. *et al.* Design of potent and selective inhibitors of *myo*-inositol 1,4,5-trisphosphate 5-phosphatase. *Biochemistry* **33**, 10763–10769 (1994).
18. Wojcikiewicz, R. J. Type I, II, and III inositol 1,4,5-trisphosphate receptors are unequally susceptible to down-regulation and are expressed in markedly different proportions in different cell types. *J. Biol. Chem.* **270**, 11678–11683 (1995).
19. De Smedt, H. *et al.* Determination of relative amounts of inositol trisphosphate receptor mRNA isoforms by ratio polymerase chain reaction. *J. Biol. Chem.* **269**, 21691–21698 (1994).
20. Bird, G. S. & Putney, J. W. Jr. Effect of inositol 1,3,4,5-tetrakisphosphate on inositol trisphosphate-activated Ca^{2+} signaling in mouse lacrimal acinar cells. *J. Biol. Chem.* **271**, 6766–6770 (1996).
21. Communi, D., Dewaste, V. & Erneux, C. Calcium-calmodulin-dependent protein kinase II and protein kinase C- mediated phosphorylation and activation of D-*myo*-inositol 1,4,5-trisphosphate 3-kinase B in astrocytes. *J. Biol. Chem.* **274**, 14734–14742 (1999).
22. De Smedt, F. *et al.* Isoprenylated human brain type I inositol 1,4,5-trisphosphate 5- phosphatase controls Ca^{2+} oscillations induced by ATP in Chinese hamster ovary cells. *J. Biol. Chem.* **272**, 17367–17375 (1997).
23. Parekh, A. B. & Penner, R. Depletion-activated calcium current is inhibited by protein kinase in RBL-2H3 cells. *Proc. Natl Acad. Sci. USA* **92**, 7907–7911 (1995).
24. Hughes, A. R., Takemura, H. & Putney, J. W. Jr. Kinetics of inositol 1,4,5-trisphosphate and inositol cyclic 1:2,4,5-trisphosphate metabolism in intact rat parotid acinar cells. Relationship to calcium signalling. *J. Biol. Chem.* **263**, 10314–10319 (1988).
25. da Silva, C. P., Emmrich, F. & Guse, A. H. Adriamycin inhibits inositol 1,4,5-trisphosphate 3-kinase activity *in vitro* and blocks formation of inositol 1,3,4,5-tetrakisphosphate in stimulated Jurkat T-lymphocytes. Does inositol 1,3,4,5-tetrakisphosphate play a role in Ca^{2+}-entry? *J. Biol. Chem.* **269**, 12521–12526 (1994).
26. Balla, T. *et al.* Agonist-induced calcium signaling is impaired in fibroblasts overproducing inositol 1,3,4,5-tetrakisphosphate. *J. Biol. Chem.* **266**, 24719–24726 (1991).
27. Riley, A. M., Mahon, M. F. & Potter, B. V. L. Rapid synthesis of the enantiomers of *myo*-inositol 1,3,4,5-tetrakisphosphate by direct chiral desymmetrization of *myo*-inositol orthoformate. *Angew. Chem. Int. Edn. Eng.* **36**, 1472–1474 (1997).
28. Yoshimura, K., Watanabe, Y., Erneux, C. & Hirata, M. Use of phosphorofluoridate analogues of D-*myo*-inositol 1,4,5-trisphosphate to assess the involvement of ionic interactions in its recognition by the receptor and metabolising enzymes. *Cell. Signal.* **11**, 117–125 (1999).
29. Worley, P. F., Baraban, J. M., Supattapone, S., Wilson, V. S. & Snyder, S. H. Characterization of inositol trisphosphate receptor binding in brain. Regulation by pH and calcium. *J. Biol. Chem.* **262**, 12132–12136 (1987).

A Toll-like receptor recognizes bacterial DNA

Hiroaki Hemmi*†, Osamu Takeuchi*†, Taro Kawai*†, Tsuneyasu Kaisho*†, Shintaro Sato*†, Hideki Sanjo*†, Makoto Matsumoto*†, Katsuaki Hoshino*†, Hermann Wagner‡, Kiyoshi Takeda*† & Shizuo Akira*†

* Department of Host Defense, Research Institute for Microbial Diseases, Osaka University and † Core Research for Evolutional Science and Technology, Japan Science and Technology Corporation, 3-1 Yamada-oka, Suita, Osaka 565-0871, Japan
‡ Institute of Medical Microbiology, Immunology and Hygiene, Technical University of Munich, Trogerstr. 9, D-81675 Munich, Germany

....

DNA from bacteria has stimulatory effects on mammalian immune cells[1-3], which depend on the presence of unmethylated CpG dinucleotides in the bacterial DNA. In contrast, mammalian DNA has a low frequency of CpG dinucleotides, and these are mostly methylated; therefore, mammalian DNA does not have immuno-stimulatory activity. CpG DNA induces a strong T-helper-1-like inflammatory response[4-7]. Accumulating evidence has revealed the therapeutic potential of CpG DNA as adjuvants for vaccination strategies for cancer, allergy and infectious diseases[8-10]. Despite its promising clinical use, the molecular mechanism by which CpG DNA activates immune cells remains unclear. Here we show that cellular response to CpG DNA is mediated by a Toll-like receptor, TLR9. TLR9-deficient (TLR9$^{-/-}$) mice did not show any response to CpG DNA, including proliferation of splenocytes, inflammatory cytokine production from macrophages and maturation of dendritic cells. TLR9$^{-/-}$ mice showed resistance to the lethal effect of CpG DNA without any elevation of serum pro-inflammatory cytokine levels. The *in vivo* CpG-DNA-mediated T-helper type-1 response was also abolished in TLR9$^{-/-}$ mice. Thus, vertebrate immune systems appear to have evolved a specific Toll-like receptor that distinguishes bacterial DNA from self-DNA.

The Toll-like receptor (TLR) family is a phylogenetically conserved mediator of innate immunity that is essential for microbial recognition[11]. Mammalian TLRs comprise a large family with extracellular leucine-rich repeats (LRRs) and a cytoplasmic Toll/interleukin (IL)-1R (TIR) homology domain. So far, six members (TLR1−6) have been reported[12-14], and two additional members have been deposited in GenBank as TLR7 and TLR8 (accession numbers AF240467 and AF246971, respectively). TLR2 and TLR4 are responsible for immune responses to peptidoglycan (PGN) and lipopolysaccharide (LPS), respectively[15-22].

By using a BLAST search, we identified an expressed sequence tag (EST) clone (AA273731; mouse) that showed high similarity with the previously identified TLRs. Using this fragment as a probe, we isolated a full-length complementary DNA from the mouse macrophage cDNA library. We also isolated the human counterpart. Sequence analysis revealed the presence of regions conserved in the TLR family, such as LRR and TIR domain (Fig. 1a, b). Therefore, we designated this gene TLR9. Northern blot analysis of various tissues indicated that mouse TLR9 transcripts were most abundantly expressed in the spleen (Fig. 1c).

To assess the biological function of TLR9, we generated TLR9$^{-/-}$ mice by homologous recombination in embryonic stem (ES) cells. The targeting vector was constructed to replace a 1.0-kb fragment of the mouse *Tlr9* gene encoding a part of LRR with a neomycin resistance cassette (*neo*) (Fig. 2a). Correctly targeted ES cell clones were micro-injected into C57BL/6 blastocysts, which contributed to transmission of the mutated allele through the germ line. We intercrossed heterozygotes to produce offspring that were homozygous for the disrupted *Tlr9* allele (Fig. 2b). The mutant mice were